J Wood Sci (2003) 49:199–209

ORIGINAL ARTICLE

Tamami Kawasaki · Kweonhwan Hwang · Kohei Komatsu
Shuichi Kawai

In-plane shear properties of the wood-based sandwich panel as a small shear wall evaluated by the shear test method using tie-rods

Received: May 9, 2001 / Accepted: June 26, 2002

Abstract The fundamental in-plane shear properties were investigated for the wood-based sandwich panel of plywood-overlaid low-density fiberboard (SW) manufactured at a pilot scale to develop it as a shear wall. The shear test method using tie-rods standardized for shear walls was applied to SW with dimensions of 260 mm square and 96 mm thick as a small shear wall and to plywood (PW) and thick low-density fiberboard (FB). The shear modulus and shear strength of PW, FB, and SW were determined. To measure the shear deformation angle, a displacement meter and strain-gauge were used. The shear moduli of PW (0.68 g/cm^3) and FB (0.25–0.35 g/cm^3) were 460 and 21–58 MPa/rad, respectively. The shear modulus of SW as a composite was analyzed. Some experimental models of SW were proposed (i.e., rigid-α, rigid-β, flexible, and semirigid models). The shear modulus of SW (0.35–0.40 g/cm^3) evaluated based on the rigid-α and semirigid models were 73–89 and 109–125 MPa/rad, respectively. The theoretical shear modulus of SW was calculated to be 110–129 MPa/rad.

Key words Shear property · Sandwich panel · Composite · Fiberboard · Plywood

Introduction

Sandwich panel consists of a lightweight core and two stiff faces.[1,2] Some commercial sandwich panels have been composed of polyurethane or polystyrene foam overlaid with oriented strand board (OSB) for thermal insulation of dwelling houses. Low-density fiberboard has adequate thermal insulation properties to substitute for conventional insulation materials,[3] and when sandwiched with veneers it was found to be viable for structural use.[4]

A wood-based sandwich panel of plywood-overlaid low-density fiberboard was manufactured in this study and in-plane shear properties were investigated to develop it as a shear wall. The shear test method for building construction[5] was modified and applied to the sandwich panel as 260 mm square, regarding it a small shear wall. The test was also applied to plywood and low-density fiberboard.

The behavior of the sandwich panel was analyzed based on some originally proposed models, and its appropriateness was examined. Shear strength was also determined.

T. Kawasaki (✉) · K. Hwang · K. Komatsu · S. Kawai
Wood Research Institute, Kyoto University, Gokasho, Uji, Kyoto 611-0011, Japan
Tel. +81-774-38-3677; Fax +81-774-38-3678
e-mail: m54247@sakura.kudpc.kyoto-u.ac.jp

Part of this report was presented at the 50th Annual Meeting of the Japan Wood Research Society, Kyoto, Japan, April 2000; and the 5th Pacific Rim Bio-Based Composite Symposium, Canberra, Australia, December 2000

Experimental

Test specimen

Sandwich panels of plywood-overlaid low-density fiberboard (SW) were manufactured. For the core of the SW, fiber from lauan (*Shorea* spp.) was used that had been commercially produced using pressurized double disk refiner (PDDR) (Hokushin Co.). The resin adhesive was commercial polymeric methylene diphenyl diisocyanate (MDI) (Mitsui Takeda Chemical Co.). The resin content was 10% solid resin of MDI based on its oven-dried fiber weight.

Plywood was used for the face material of SW. It was commercially produced from weather- and boil-proof plywood (type special)[6] of 9 mm thickness. It consisted of three plies of 3-mm layers of Japanese larch (*Larix gmelini* Gordon), with an average density of 0.68 g/cm^3. Before pressing, the MDI (UL-4811, Gun-ei Kagaku Kogyo Co.) was spread for internal bonding between the core and the face of the SW at 75 g/m^2 (solid basis) for a bonding layer.

The assembled fiber mat with faces was pressed once using the steam-injection pressing machine, heating from both sides.[7] The target density range for SW was 0.35–0.40 g/cm^3. The target thickness of SW was 100 mm, and the aver-

age total thickness of the SW was 96 mm. Hence the core thickness was 78 mm. Figure 1 shows the SW sample. The density profile in the SW core was flat throughout the thickness. SW specimens of 260 × 260 × 96 mm were prepared for the shear test.

The low-density fiberboard (FB) was manufactured similarly, with a core of SW. The target density range for FB was 0.25–0.35 g/cm^3, the same core density as that of SW. The average thickness of the FB was 96 mm. FB specimens of 260 × 260 × 96 mm were prepared. Specimens of the raw material of the plywood (PW) were prepared with dimensions of 260 × 260 × 9 mm.

Shear test method

The shear test method of Japanese Industrial Standard (JIS) A1414 (method A using tie-rods),[5] was applied to the SW, with some modifications of the specimen preparation and apparatus. This method is usually used for full-scale shear wall (i.e., 900 × 2400 mm or more). A specimen of 260 mm square was regarded as a small shear wall. The test was also applied to PW and FB.

Fig. 1. Sample of the sandwich panel of plywood-overlaid low-density fiberboard (SW). Total board thickness is 96 mm including a 78 mm thick core and 9 mm thick faces. The density of the specimen is 0.35 g/cm^3

In this connection, there are standard methods for boards.[6,8,9] Some studies have been reported, using these methods but they have been on higher density board.[10–17] Research using lower-density fiberboard has been slow to evolve.

The test conditions are summarized in Table 1. Figure 2 gives the details for preparing the specimen. Four pieces of reinforcing frame of laminated wood (*Pseudotsuga menziesii* Franco) were glued to both lateral surfaces of the specimen at the top and bottom edges (top and bottom frames) using epoxy resin adhesive. The frame size was 60 × 60 × 600 mm. Exceptionally, the width of the bottom frame for PW was 105 mm for convenience so the bolt could be inserted in the same hole as in the other cases (using a frame 60 mm width gives the same results). These frames were also fastened to the specimens for reinforcement using mechanical fasteners such as a lag screw, bolt, nail, and screw nail.

The details of the combination of fastener types used for the top and bottom frames are indicated in Table 1 and Fig. 2. Moderate numbers and sizes of the fastener were selected; they were not excessive to avoid crushing or tearing the specimen before loading took place. Any of the specimens could provide satisfactory shear deformation corresponding to the applied load. The fasteners could hold the specimen without breaking or being pulled out. The contact area of the fasteners was sufficient even in the fiber materials with larger numbers and sizes.

The outside view of the apparatus of the shear test using tie-rods is illustrated in Fig. 3. The load was applied to the top frames. One tie-rod was used for the monotonic-push (MP) load test (Fig. 3A), and two tie-rods were used for the push-and-pull cyclic (PPC) load test (Fig. 3B). The diameter of the tie-rod was 13 mm. A top-roller and two steel plates piled up over the specimen were fixed lightly to the base plate of steel using the tie-rod. The bottom reinforcing frames were fastened tightly to the base plate with four anchor bolts of 16 mm diameter (Fig. 3C,D). Two adjustable

Table 1. Test conditions

Sample type	Sample (pieces)	Load	Tie-rod (pieces)	Direction	Fastener type (pieces)		Size of lag screw (mm)
					Top frames	Bottom frames	
1	SW (2)	MP	1	90°	L (5) + B (1)	L (5)	16 × 150
2	SW (1)	MP	1	90°	L (5) + B (1) + SN (16)	L (5) + SN (12)	16 × 150
3	SW (1)	MP	1	90°	L (5) + B* (1) + SN (8) + N (4)	L (5) + SN (4) + N (8)	16 × 150
4	SW (4)	PPC	2	0°	L (10)	L (10)	10 × 100
5	SW (3)	PPC	2	90°	L (10)	L (10)	10 × 100
6	PW (3)	MP	1	0°	L (5)	B (5)	12 × 125
7	PW (3)	MP	1	90°	L (5)	B (5)	12 × 125
8	FB (6)	MP	1	–	L (5) + B (1)	L (5)	16 × 150

Direction, setting direction of the sample surface grain to load; MP, monotonic-push load; PPC, push-and-pull cyclic load; L, lag screw; B, bolt (12 × 240 mm); N, nail (5 × 150 mm); SN, screw nail (5 × 150 mm); B*, bolt was connected off sample with frame.
The "plus" symbol in the fastener type means a combination of fasteners. The number of each kind of fastener (pieces) is indicated in parentheses after the fastener type. The length of the fastener means the length under the stopper (effective length)

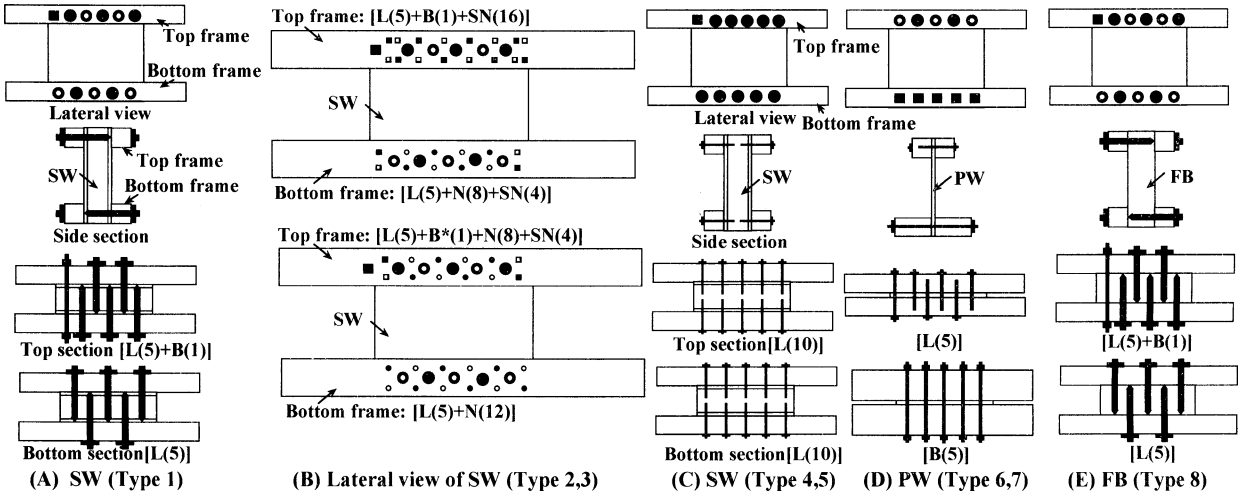

Fig. 2. Examples of the fastener type (refer to Table 1) indicated in parentheses for SW (**A–C**), plywood (*PW*) (**D**), and fiberboard (*FB*) (**E**). *Large circles*, *L*; *large squares*, *B*; *small circles*, *N*; *small squares*, *SN*. Fasteners were inserted in the frames in front (*filled symbols*) and back (*open symbols*)

Fig. 3. Apparatus of the shear test under the monotonic-push (**A**) and push-and-pull cyclic (**B**) load and its view from the side cross section of SW and FB (**C**) and PW (**D**). Examples of the setting direction of the specimen, where the surface grain is parallel (**A**) or perpendicular (**B**) to the applied load direction

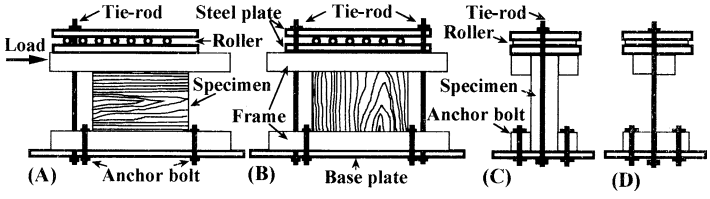

Fig. 4. Location of the measurement points of the displacement meters for the side cross section of the specimens (**A**) and on the bottom frame (**B**). The location of the measurement points of the rosette strain-gauges (**C**). Points (*p*)–(*t*) are on the lateral surface of the specimen, and point (*p′*) is centered on the other lateral surface of the specimen

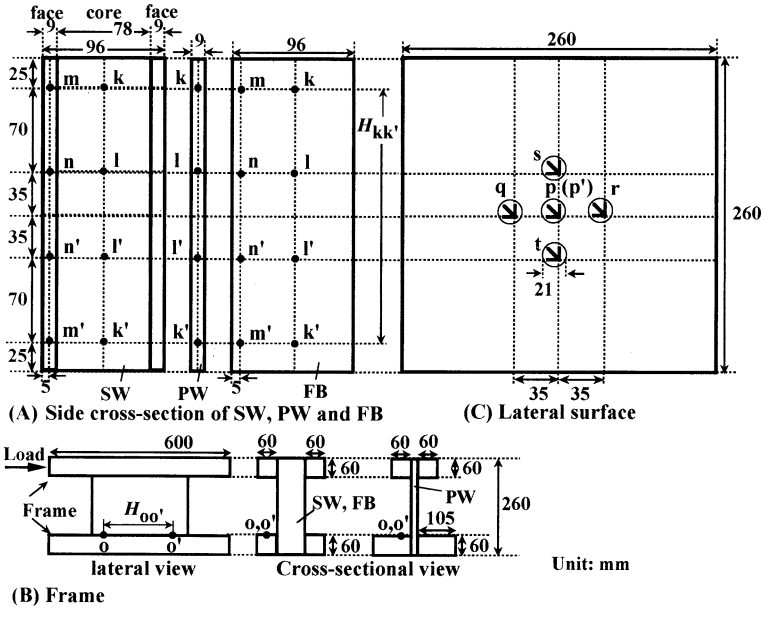

lateral-rollers of 30 mm diameter and 100 mm length made from hard plastic were set aside on the lateral surfaces of the top frames. This was for lateral support to restrict lateral deflection, allowing movement of the specimen along a direction parallel to the applied load direction without frictional restraint.

Two setting directions of the specimen were compared (Table 1): The surface grain of the plywood veneer was taken parallel (0°) or perpendicular (90°) to the applied load direction for SW and PW. The 90° direction was taken in all cases because it is considered to be more suitable for shear wall. The setting directions are indicated in Fig. 3A,B.

For SW, the load test applied was MP for four pieces and PPC for the other seven pieces. For both PW and FB, the MP load test was applied to six pieces each. Although the PPC load test is not yet standardized, it prevails in the field of testing for full-scale shear wall (e.g., for earthquakes). The turning point of the PPC load was considered to occur

when the displacement (measured at point k in Fig. 4) indicated 1/300, 1/120, 1/60, 1/30, and 1/10 of the sample depth of 260 mm. Loading was continued until complete failure.

Measurement of shear deformation angle

The shear deformation angle of the whole specimen at an early stage must be measured to determine the shear modulus. Generally, the standard for a shear wall[5] makes it a rule to use a displacement meter, whereas the standard for structural panels[8] uses a strain-gauge. With the former method, some displacement meters are set at various places to cover a large portion of the specimen. With the latter method, the strain-gauge covers a relatively limited portion of the specimen. Such differences in measuring devices and locations are not a problem when the deformation can be assumed to be uniform over the whole material. If it is not uniform, these differences must be taken into consideration.

This problem cannot be avoided for the composite materials of sandwich panels with a low-density core or for lower-density fiberboard. Therefore, in this study shear deformation angles were measured to understand as much of the behavior of SW as possible using both devices (displacement meter and strain-gauge). We also examined the differences in their results.

Using the displacement meter

The shear deformation angle of SW was measured using displacement meters, referring to the standard for the wall.[5] The location is shown in Fig. 4A,B. Thin plastic plates of 5–30 mm square were placed on the measurement points. A pair of displacement meters were set horizontally at points k and k′ in Fig. 4A at a distance of $H_{kk'}$. The shear deformation angle including the rotation angle was defined as follows.

$$\gamma_{kk'} = \frac{\delta_k - \delta_{k'}}{H_{kk'}} \tag{1}$$

where δ_k and $\delta_{k'}$ denote the displacements of the respective points k and k′. Another pair of displacement meters were set vertically at points o and o′ (Fig. 4B) at a distance of $H_{oo'}$ on the bottom frame. The rotation angle was defined as follows.

$$\gamma_R = \frac{\delta_o - \delta_{o'}}{H_{oo'}} \tag{2}$$

where δ_o and $\delta_{o'}$ denote the displacements of the respective points o and o′. The shear deformation angle without the rotation angle for the pair of points k and k′ was defined as follows.

$$\gamma_k = \gamma_{kk'} - \gamma_R \tag{3}$$

For some specimens, another pair of points l and l′ were taken to compare with the γ_k (Fig. 4A). The other two pairs of points m and m′ and points n and n′ were taken 5 mm from edge; they were within the face of SW. Similar measurements were made for PW and FB.

Using the strain-gauge

The shear deformation angle of SW was measured using a strain-gauge, referring to the standard for the structural panel[8] with some modifications of the strain-gauge type and length. The rectangular rosette strain-gauges with a gauge length of 10 mm grid on paper-base with a diameter of 21 mm (K-10-120-B4-11; Kyowa Dengyo Co.) were bonded at the measuring points at the center of both lateral surfaces of the specimen using instant cement. As shown in Fig. 4C, points p and p′ were located at the center of each lateral surface of the specimen. The shear deformation angle without rotation angle at point p was determined as follows.

$$\gamma_p = 2\varepsilon_{45} - (\varepsilon_0 + \varepsilon_{90}) \tag{4}$$

where ε_0, ε_{45}, and ε_{90} denote the strain at point p along directions 0°, 45°, and 90° to the load direction, respectively. The $\gamma_{p'}$ for point p′ was determined in the same manner. For some specimens to check with p, another four points (from q to t) were taken on the lateral surface (Fig. 4C). The lateral surface around the measurement points on the face plywood of SW were ground smooth with sandpaper in advance. No knots were found on the surface of the plywood. PW was treated similarly. The surface of FB was smooth and hard enough to bond the strain-gauge.

Results and discussion

Evaluation of shear modulus

Shear deformation angle

For SW, the shear deformation angles evaluated using the displacement meter were compared within the pairs of points k to n. The difference between them was not significant in any specimen. Therefore the value at k was regarded as the representation for each specimen. On the other hand, the shear deformation angles of SW evaluated using the strain-gauge were compared within points p to t. The difference between them was not significant in any specimen. No significant trend was observed. Hence the value at p was regarded as representative for these specimens. Similar trends were observed for PW and FB.

The γ_k as representive was described again as follows.

$$\gamma_\alpha = \gamma_k \tag{5}$$

According to the standard,[8] the γ_p and $\gamma_{p'}$ values were averaged and defined as follows.

$$\gamma_\beta = \frac{(\gamma_p + \gamma_{p'})}{2} \tag{6}$$

The γ_α values for SW, PW, and FB were defined as $\gamma_{SW\alpha}$, $\gamma_{PW\alpha}$, and $\gamma_{FB\alpha}$, respectively. The $\gamma_{PW\beta}$, $\gamma_{FB\beta}$, and $\gamma_{SW\beta}$ values were defined similarly for γ_β.

Load-shear deformation angle curve

Thus, derived γ_α and γ_β were observed in relation to the total applied load, P. Examples of the P/γ_α and P/γ_β curves for SW, PW, and FB under the MP load are shown in Fig. 5A and B, respectively. The P/γ_α and P/γ_β curves for SW under the PPC load are shown in Fig. 5C and D, respectively.

Under the MP load, the P/γ_α curves, for each SW, PW, and FB specimen corresponded to the movement of the specimen almost until the final fracture. For each SW specimen under the PPC load, P/γ_α gave the typical looping curve, which is usually observed with the wall test.[5] The P/γ_β data were almost linear in the tests with both types of loading. It followed deformation during the early stage. In the later stage, near the final fracture, the gauge was broken.

Shear modulus of PW and FB

To evaluate the shear modulus of SW, those of PW and FB were investigated first. The slopes of the linear portion of the P/γ_α and P/γ_β curves for each specimen were defined as K_α and K_β, respectively.

$$K_\alpha = \frac{P}{\gamma_\alpha},\ K_\beta = \frac{P}{\gamma_\beta} \tag{7}$$

The P/γ_α and P/γ_β data used in the calculation were within the proportional limits, where the load was less than the P at the γ_α was 1/300 radian. The K_α and K_β values for PW and FB were described as $K_{PW\alpha}$, $K_{PW\beta}$, $K_{FB\alpha}$, and $K_{FB\beta}$, respectively.

The K_α and K_β values for PW and FB in relation to board density are shown in Fig. 6. The setting direction and fastener types are not distinguished in Fig. 6. The effect of the setting direction was not significant. The effect of various fastener types was satisfactorily negligible. In PW (0.68 g/cm^3), the average value of $K_{PW\alpha}$ was 1.1 MN/rad and that of $K_{PW\beta}$ was 1.3 MN/rad. In FB the $K_{FB\alpha}$ depended on board density, and the regression curve of involution function ($y = 34x^{3.0}$, $R^2 = 0.95$, where R^2 is correlation coefficient) was fitted (Fig. 6). Hence, the $K_{FB\alpha}$ of FB (0.25–0.35 g/cm^3) was 0.5–1.5 MN/rad.

For PW, the $G_{PW\alpha}$ and $G_{PW\beta}$ values were defined as follows.

$$G_{PW\alpha} = \frac{K_{PW\alpha}}{A_{PW}},\ G_{PW\beta} = \frac{K_{PW\beta}}{A_{PW}} \tag{8}$$

where the A_{PW} is the shear sectional area of PW. These values are shown in Fig. 7. The average $G_{PW\alpha}$ (0.68 g/cm^3) value was 460 MPa/rad, and that of $G_{PW\beta}$ was 550 MPa/rad. The difference between the $G_{PW\alpha}$ and $G_{PW\beta}$ was not significant although $G_{PW\beta}$ was somewhat higher than $G_{PW\alpha}$. It was because PW was relatively stiff, uniform material. The shear force transmitted throughout the grain of the veneer effectively over the whole specimen. Hence the measuring location had no effect. The $G_{PW\alpha}$ and $G_{PW\beta}$ approximated the shear modulus of the entire specimen well.

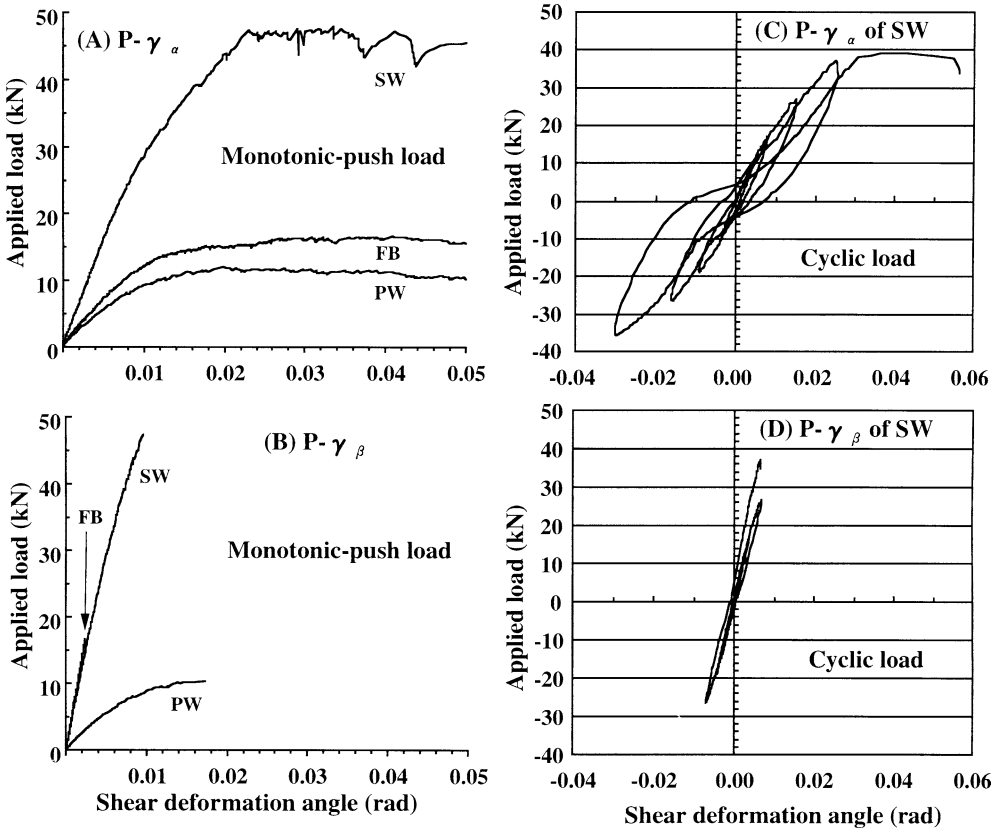

Fig. 5. Examples of the P–γ_α and P–γ_β curves. The specimens in (**A**) and (**B**) are SW (0.43 g/cm^3), PW (0.69 g/cm^3), and FB (0.38 g/cm^3) under the monotonic-push load. The setting direction of SW and PW is perpendicular. The specimen in (**C**) and (**D**) is SW (0.41 g/cm^3) in the parallel setting direction under the push-and-pull cyclic load

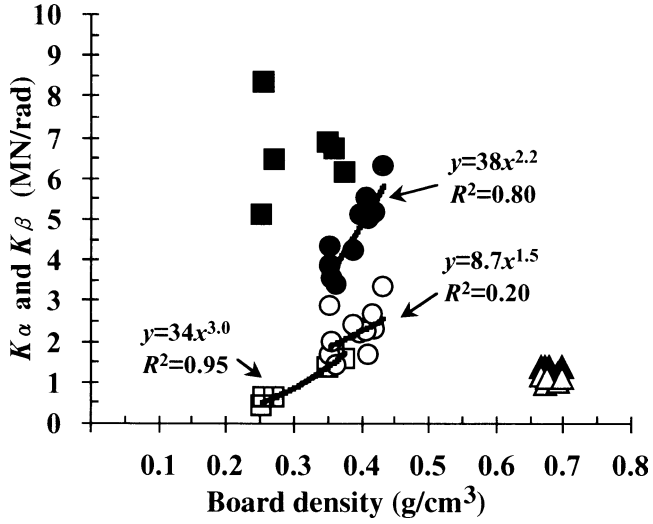

Fig. 6. Values of K_α (*open symbols*) and K_β (*filled symbols*) of SW (*circles*), PW (*triangles*), and FB (*squares*) in relation to the board density. *Solid lines*, regression curves for $K_{SW\alpha}$, $K_{SW\beta}$, and $K_{FB\alpha}$

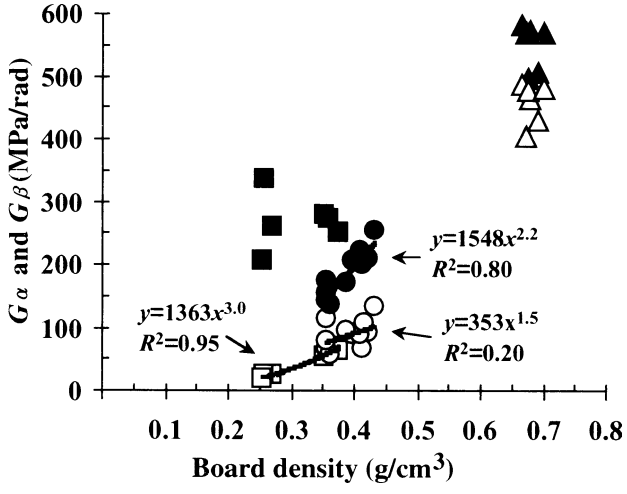

Fig. 7. Values of G_α (*open symbols*) and G_β (*filled symbols*) of SW (*circles*), PW (*triangles*), and FB (*squares*) in relation to board density. *Solid lines*, regression curves for $G_{SW\alpha}$, $G_{SW\beta}$, and $G_{FB\alpha}$

For FB, the $G_{FB\alpha}$ and $G_{FB\beta}$ values were defined similarly.

$$G_{FB\alpha} = \frac{K_{FB\alpha}}{A_{FB}},\ G_{FB\beta} = \frac{K_{FB\beta}}{A_{FB}} \tag{9}$$

where the A_{FB} is the shear sectional area of FB. A difference between $G_{FB\alpha}$ and $G_{FB\beta}$ was observed: $G_{FB\beta}$ was much higher than $G_{FB\alpha}$. The $G_{FB\alpha}$ was dependent on the board density. The $G_{FB\alpha}$ increased with the increase in board density. The $G_{FB\alpha}$ at densities of 0.25, 0.30, and 0.35 g/cm^3 were 21, 37, and 58 MPa/rad, respectively, according to the regression curve ($y = 1363x^{3.0}$, $R^2 = 0.95$) (Fig. 7).

According to Wong,[18] the shear modulus of fiberboard with a density of 0.3–0.4 g/cm^3 evaluated by the torsion method is 30–36 MPa, and that of particleboard (0.3–0.4 g/cm^3) evaluated by the tapping method is 22–96 MPa. Compared to these results, the $G_{FB\alpha}$ is considered to be highly reliable as the shear modulus of FB. $G_{FB\beta}$ seemed independent of board density and was around 200–300 MPa/rad (Fig. 7). This value is high considering the low board density.

One reason is the construction of FB with low-density fiberboard, which is a uniform fibrous material. The shear force transmitted effectively throughout the specimen through the many contact points of a large number of fibers. Shear deformation was elastic during the early stage and seemed uniform macroscopically. No local fractures were observed, although it is possible that there were microscopic local fractures that caused the whole deformation. The limited measured location remained stable compared to the overall behavior. Hence $G_{FB\beta}$ was negligible for the purpose of this study. Further investigation of the distribution of shear deformation within a fiberboard is left to future studies.

Evaluation of the shear modulus of SW

The $K_{SW\alpha}$ and $K_{SW\beta}$ values are shown in Fig. 6. There was a difference between them. Both values depended strongly on board density (core density), unlike FB. According to the regression curves fitted for $K_{SW\alpha}$ ($y = 8.7x^{1.5}$, $R^2 = 0.20$) and $K_{SW\beta}$ ($y = 38x^{2.2}$, $R^2 = 0.80$), the $K_{SW\alpha}$ was 1.8–2.2 MN/rad, and the $K_{SW\beta}$ was 3.8–5.1 MN/rad for the density range 0.35–0.40 g/cm^3 (Fig. 6).

The differences between $K_{SW\alpha}$ and $K_{SW\beta}$ were derived from the difference between $\gamma_{SW\alpha}$ and $\gamma_{SW\beta}$. As discussed above, the shear deformation angles measured in a section of the face were the same as those of the core but were different from those on the surface of the face. The difference was seen in the face materials. Location had no effect in a specimen of plywood only. One reason for this was the sandwich construction, with two stiff faces and a fibrous core. Under shear force these elements behaved neither together nor independently. Such an interaction made the behavior of SW, as a composite, unique.

The hypotheses should be examined theoretically. For example, there is a method for calculating the divided shear force in the horizontal diaphragm (floor or ceiling between shear walls) when designing wooden house construction.[19] It deals with rigid and flexible floors. Therefore, it is set up for sandwich panel construction so the shear modulus of SW can be analyzed.

Analysis of the shear modulus of SW

To understand the shear behavior of SW, the measured values of $\gamma_{SW\alpha}$ and $\gamma_{SW\beta}$ are regarded as partial contributors. To examine their contribution to the overall behavior, some experimental models are proposed. Experimental shear moduli can be derived from each model. On the other hand, a theoretical model using the shear moduli of PW and FB can be calculated. These values are compared, and it can be determined which experimental model more accurately simulates SW behavior.

To examine the relation between deformation and shear force in the shear section, models of SW shear sections are considered (Fig. 8). The factors of load (P), shear modulus

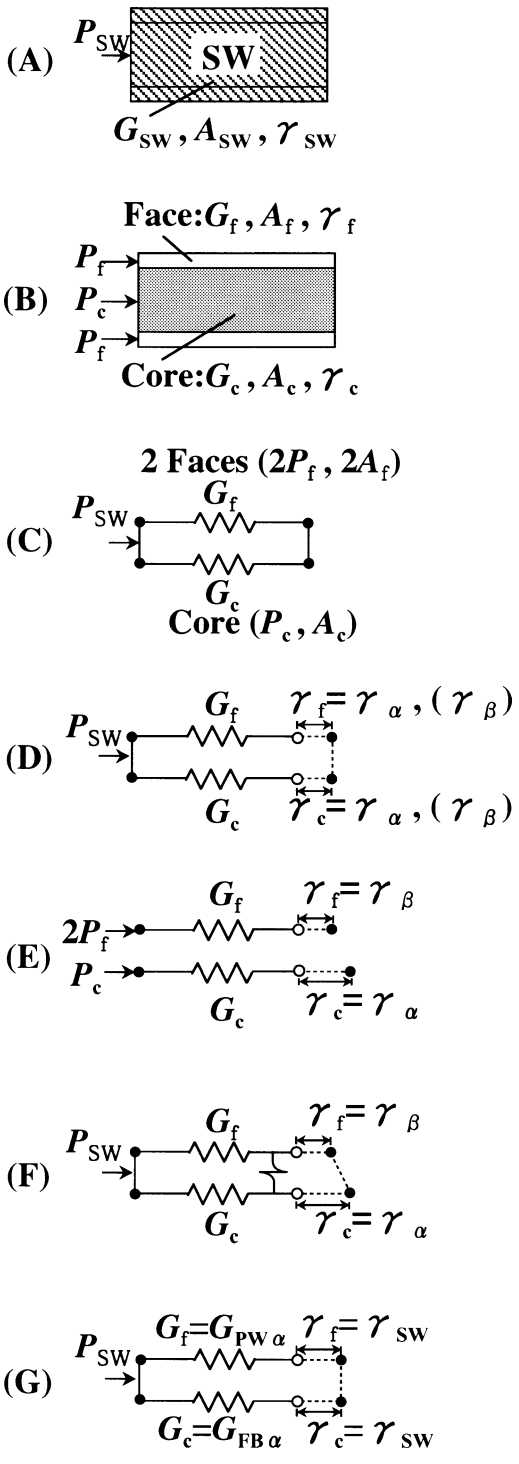

Fig. 8. Models of shear section of SW. Diagrams of the composite body (**A**) and elements (**B**). Spring models of basic (**C**) and experimental models [rigid (**D**), flexible (**E**), and semirigid (**F**) models] and of the theoretical model (**G**)

(G), shear area (A), and shear deformation angle (γ) are assigned to SW as a composite (Fig. 8A) and its elements (Fig. 8B), respectively. Subscript SW indicates the composite body of SW, and subscripts c and f indicate the core and one of the faces, respectively. Generally,

$$P_f = G_f A_f \gamma_f \tag{10}$$

$$P_c = G_c A_c \gamma_c \tag{11}$$

$$P_{sw} = P_c + 2P_f \tag{12}$$

Experimental models of SW

The experimental shear modulus of SW was evaluated first. The spring model is considered (Fig. 8C). It consists of two elastic springs; one indicates the two faces and the other indicates the core. Factors $2P_f$, G_f, $2A_f$, and γ_f are assigned to the two faces. Factors P_c, G_c, A_c, and γ_c, are assigned to the core. The relations between the values for γ_c and γ_f and the measured values for $\gamma_{SW\alpha}$ and $\gamma_{SW\beta}$ are assumed as follows.

$$\gamma_c = \gamma_{SW\alpha},\ \gamma_f = \gamma_{SW\alpha} \tag{13}$$

$$\gamma_c = \gamma_{SW\beta},\ \gamma_f = \gamma_{SW\beta} \tag{14}$$

$$\gamma_c = \gamma_{SW\alpha},\ \gamma_f = \gamma_{SW\beta} \tag{15}$$

Equations 13 and 14 indicate that the effect of the measuring location is ignored in the shear section. They assume that SW is rigid material, and that the rigid model is derived (Fig. 8D). The location effect is considered in Eq. 15, where SW is assumed to be rather flexible, and the flexible model (Fig. 8E) and semirigid model (Fig. 8F) are derived from it. The $\gamma_{SW\alpha}$ and $\gamma_{SW\beta}$ values are regarded as partial to some extent. To evaluate the G_{SW} for each model, G_c and G_f are calculated. G_c can be obtained from Eqs. 10–12.

$$G_c = \frac{P_{SW} - 2G_f A_f \gamma_f}{A_c \gamma_c} \tag{16}$$

The G_c and G_f values for each model are derived as follows.

Rigid model. When it is supposed that the composite behaves like a completely unified rigid material, the "rigid model" is proposed (Fig. 8D). In the "rigid model" the shear deformations of the elements correspond completely (Eqs. 13 and 14). The rigid models based on Eqs. 13 and 14 are called the "rigid-α model" and the "rigid-β model," respectively. They satisfy Eq. 17.

$$\gamma_c = \gamma_f \tag{17}$$

The G_c based on Eqs. 13 and 14 is defined as $G_{cR\alpha}$ and $G_{cR\beta}$, respectively. From Eq. 16,

$$G_{cR\alpha} = \frac{K_{SW\alpha} - 2G_f A_f}{A_c} \tag{18}$$

$$G_{cR\beta} = \frac{K_{SW\beta} - 2G_f A_f}{A_c} \tag{19}$$

The G_f values in these models are taken to be 460 MPa/rad considering $G_{PW\alpha}$.

Flexible model. When it is supposed that each element of the core and face behaves separately and independently,

the "flexible model" is proposed (Fig. 8E). In the "flexible model" it is supposed that the shear deformations of the elements are different (Eq. 15), and that the portion of load is in proportion to the shear sectional area (Eqs. 20 and 21).

$$P_c = \frac{P_{SW} A_c}{A_{SW}} \tag{20}$$

$$P_f = \frac{P_{SW} A_f}{A_{SW}} \tag{21}$$

The G_c value obtained from Eqs. 11 and 20 is defined as G_{cF}.

$$G_{cF} = \frac{K_{\alpha SW}}{A_{SW}} \tag{22}$$

In this model G_f is calculated from $K_{SW\beta}$ divided by A_{SW}. It is 144–255 MPa/rad.

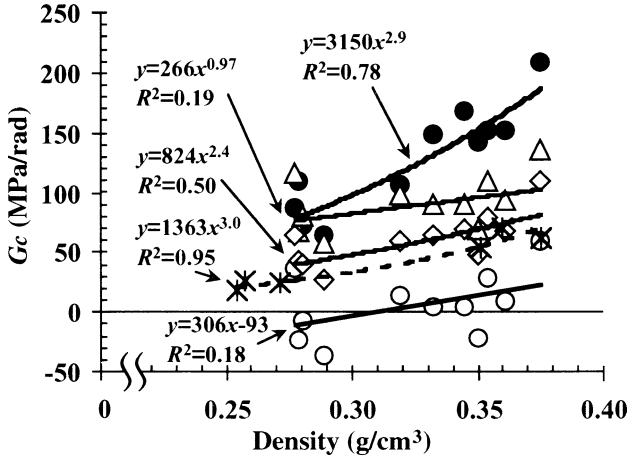

Fig. 9. Values of $G_{cR\alpha}$ (*open circles*), $G_{cR\beta}$ (*filled circles*), G_{cF} (*open triangles*), and G_{cS} (*open diamonds*) in relation to the core density of SW and their regression curves (*solid lines*). *Dashed line,* regression curve of the $G_{FB\alpha}$ (*asterisk*) in relation to the density of FB

Semirigid model. When it is supposed that the behaviors of the elements are not the same but are dependent on each other, the "semirigid model" is proposed (Fig. 8F). The dependent interaction between the faces and core is expressed as the shear spring in Fig. 8F. In the "semirigid model" it is supposed that the shear deformations of the core and face are different based on Eq. 15. The G_c obtained from Eq. 16 is defined as G_{cS}.

$$G_{cS} = \frac{1 - 2G_f A_f \dfrac{1}{K_{SW\beta}}}{A_c \dfrac{1}{K_{SW\alpha}}} \tag{23}$$

In this model the G_f value is taken to be 460 MPa/rad.

Shear modulus of the core

Each G_c is examined if it approximates the shear modulus of fiberboard. The core density is 0.28–0.33 g/cm^3 for SW with a board density of 0.35–0.40 g/cm^3. The $G_{cR\alpha}$, $G_{cR\beta}$, G_{cF}, and G_{cS} are shown in relation to the core density of SW in Fig. 9. The values of G_c depend on the core density. The regression curves (solid lines) were fitted for $G_{cR\alpha}$ ($y = 306x - 93$, $R^2 = 0.18$), for $G_{cR\beta}$ ($y = 3150x^{2.9}$, $R^2 = 0.78$), for G_{cF} ($y = 266x^{0.97}$, $R^2 = 0.19$), and for G_{cS} ($y = 824x^{2.4}$, $R^2 = 0.50$). The shear modulus is thought to depend increasingly on board density similarly to the other mechanical board properties. Therefore the involution function was applied. A straight line was fitted to $G_{cR\alpha}$ instead, as it included a minus value. According to the curves (0.28–0.33 g/cm^3), $G_{cR\alpha}$ ranges from −7 to +8 MPa, though the minus value is impossible; $G_{cR\beta}$ is 79–126 MPa/rad; G_{cF} is 77–91 MPa/rad, and G_{cS} is 39–58 MPa/rad, as shown in Table 2.

The $G_{FB\alpha}$ is given in relation to the density of FB (dashed line, $y = 1363x^{3.1}$, $R^2 = 0.95$). $G_{FB\alpha}$ is 30–49 MPa/rad at the density range. The value of G_c was compared with that of $G_{FB\alpha}$. $G_{cR\alpha}$ is less than 16% of $G_{FB\alpha}$. $G_{cR\beta}$ is 260%. G_{cF} is 190%–260%. G_{cS} is 120%–130%. Therefore, G_{cS} is nearest

Table 2. Results of the analysis of shear modulus of SW

Sample			MPa/rad	Density (g/cm^3)			
PW		$G_{PW\alpha}$	460	0.68			
FB		$G_{FB\alpha}$	30	0.28			
			49	0.33			
Model			Sandwich panel			Core	
			MPa/rad	Board density (g/cm^3)		MPa/rad	Core density (g/cm^3)
SW	Rigid-α	$G_{SWR\alpha}$	73	0.35	$G_{cR\alpha}$	−7	0.28
			89	0.40		8	0.33
	Rigid-β	$G_{SWR\beta}$	154	0.35	$G_{cR\beta}$	79	0.28
			206	0.40		126	0.33
	Flexible	G_{SWF}	90	0.35	G_{cF}	77	0.28
			110	0.40		91	0.33
	Semirigid	G_{SWS}	109	0.35	G_{cS}	39	0.28
			125	0.40		58	0.33
	Theoretical	G_{SWT}	110	0.35			
			129	0.40			

PW, plywood; FB, thick, low-density fiberboard; SW, wood-based sandwich panel of plywood-overlaid low-density fiberboard; *G*, shear modulus

to $G_{FB\alpha}$. These values are examined again together later with G_{SW}.

Experimental shear modulus of SW

Using each pair of G_c and G_f obtained in the above, G_{SW} for each model is calculated on the basis of the strain energy stored in the whole specimen. Under the proportional limit, the strain energy U is

$$U = \frac{P\delta}{2} = \frac{P^2 D}{2GA} \tag{24}$$

where D denotes the depth of the specimen. There is the following relation for a sandwich panel.

$$U_{SW} = U_c + 2U_f \tag{25}$$

where the U_{SW}, U_c, and U_f denote the U of a sandwich panel, core, and a face, respectively. Substituting Eq. 24 for Eq. 25, and from Eqs. 10 and 11, G_{SW} is derived as follows.

$$G_{SW} = \frac{1}{A_{SW}\left(\frac{G_c A_c \gamma_c^2}{P_{SW}^2} + \frac{2G_f A_f \gamma_f^2}{P_{SW}^2}\right)} \tag{26}$$

The G_{SW} for each experimental model is derived as follows. In the rigid-α model Eq. 26 becomes

$$G_{SWR\alpha} = \frac{1}{A_{SW}\left(\frac{G_{cR\alpha} A_c}{K_{SW\alpha}^2} + \frac{2G_f A_f}{K_{SW\alpha}^2}\right)} \tag{27}$$

where $G_{SWR\alpha}$ denotes the G_{SW} in the rigid-α model. For the other models, the G_{SW} are defined as follows.

$$G_{SWR\beta} = \frac{1}{A_{SW}\left(\frac{G_{cR\beta} A_c}{K_{SW\beta}^2} + \frac{2G_f A_f}{K_{SW\beta}^2}\right)} \tag{28}$$

$$G_{SWF} = \frac{1}{A_{SW}\left(\frac{G_{cRF} A_c}{K_{SW\alpha}^2} + \frac{2G_f A_f}{K_{SW\beta}^2}\right)} \tag{29}$$

$$G_{SWS} = \frac{1}{A_{SW}\left(\frac{G_{cRS} A_c}{K_{SW\alpha}^2} + \frac{2G_f A_f}{K_{SW\beta}^2}\right)} \tag{30}$$

where the $G_{SWR\beta}$, G_{SWF}, and G_{SWS} denote G_{SW} in the rigid-β, flexible, and semirigid models, respectively. The $G_{SWR\alpha}$ and $G_{SWR\beta}$ values are consequently defined in Eq. 31.

$$G_{SWR\alpha} = \frac{P}{\gamma_{SW\alpha} A_{SW}},\ G_{SWR\beta} = \frac{P}{\gamma_{SW\beta} A_{SW}} \tag{31}$$

These $G_{SWR\alpha}$, $G_{SWR\beta}$, G_{SWF}, and G_{SWS} values are shown in Fig. 10. As they depended increasingly on board density, the regression curves (solid lines) of involution function were fitted for $G_{SWR\alpha}$ ($y = 353x^{1.5}$, $R^2 = 0.20$), $G_{SWR\beta}$ ($y = 1548x^{2.2}$, $R^2 = 0.80$), G_{SWF} ($y = 435x^{1.5}$, $R^2 = 0.20$), and G_{SWS} ($y = 312x^{1.0}$, $R^2 = 0.22$). According to these curves, the values of $G_{SWR\alpha}$ (0.35 and 0.40 g/cm^3) are 73 and 89 MPa/rad (Table 2); those of $G_{SWR\beta}$ are 154 and 206 MPa/rad; those of G_{SWF} are 90 and 110 MPa/rad; and those of G_{SWS} are 109 and 125 MPa/rad, respectively.

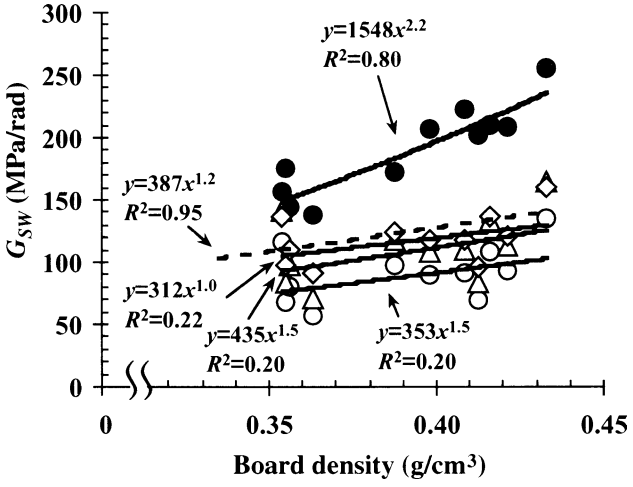

Fig. 10. Values of $G_{SWR\alpha}$ (*open circles*), $G_{SWR\beta}$ (*filled circles*), G_{SWF} *(open triangles),* and G_{SWS} (*open diamonds*) and their regression curves (*solid lines*). *Dashed line*, regression curve for the calculated values of G_{SWT}

Theoretical model of SW

To calculate the theoretical shear modulus of SW, consider the theoretical model (Fig. 8G), where it is assumed that:

$$\gamma_c = \gamma_f = \gamma_{SW} \tag{32}$$

Generally,

$$P_{SW} = G_{SW} A_{SW} \gamma_{SW} \tag{33}$$

Using Eqs. 16, 32, and 33, the theoretical shear modulus of SW is defined as G_{SWT}.

$$G_{SWT} = \frac{G_c A_c + 2G_f A_f}{A_{SW}} \tag{34}$$

The values of $G_{FB\alpha}$ and $G_{PW\alpha}$ (460 MPa/rad) are substituted for G_c and G_f in Eq. 24, respectively. Then the G_{SWT} is calculated, and the regression curve of involution function is fitted to G_{SWT} ($y = 387x^{1.2}$, $R^2 = 0.95$, dashed line), as shown in Fig. 10 in relation to the calculated board density of SW. Accordingly, G_{SWT} is 110–129 MPa/rad at a density range of 0.35–0.40 g/cm^3.

Comparison with theoretical shear modulus of SW

The $G_{SWR\alpha}$, $G_{SWR\beta}$, G_{SWF}, and G_{SWS} values (solid lines) are compared with G_{SWT} ($y = 387x^{1.2}$, $R^2 = 0.95$, dashed line) in Fig. 10. G_{SWT} is 110 and 129 MPa/rad (0.35 and 0.40 g/cm^3). According to the regression curves at densities of 0.35 and

0.40 g/cm^3, $G_{SWR\alpha}$ is 67% and 69% of G_{SWT}, respectively, and $G_{SWR\beta}$ is 140% and 160%. G_{SWF} is 82% and 85%, and G_{SWS} is 99% and 97%.

The above results are summarized considering both G_{SW} and G_c. The rigid-α model gives moderate simulation, because $G_{SWR\alpha}$ is about 70% of G_{SWT}, and $G_{cR\alpha}$ is less than 16% of $G_{FB\alpha}$. The rigid-β model is not appropriate because $G_{SWR\beta}$ values are 140%–160% of G_{SWT}, and $G_{cR\beta}$ is 260% of $G_{FB\alpha}$. In the flexible model, G_{SWF} is nearer G_{SWT} (more than 80% of G_{SWT}), but it is an imbalance that G_{cF} is 190%–260% of $G_{\alpha FB}$, and G_{fF} was much lower than G_{PW}. The semirigid model gave the closest simulation, because G_{SWS} approximates G_{SWT} (almost 100% of G_{SWT}), and G_{cS} is closest to $G_{FB\alpha}$ (120%–130% of $G_{FB\alpha}$).

As a result, the measured values of $\gamma_{SW\alpha}$ and $\gamma_{SW\beta}$ gave major and local contribution to the overall behavior, respectively, in SW. The shear behavior of SW was similar to that of the rigid-α model basically. The semirigid model was a better approach when taking local behavior into consideration, as it gave a closer approximation to the theoretical value. Further investigation of the interaction between the core and faces will be helped by determining the partial distribution of loading and its profile within SW.

Shear modulus of SW

The shear moduli of PW and FB were evaluated by $G_{PW\alpha}$ and $G_{FB\alpha}$, respectively, as shown in Fig. 11. The shear modulus of PW (0.68 g/cm^3) was 460 MPa/rad, and that of FB (0.25–0.35 g/cm^3) was 21–58 MPa/rad.

The $G_{SWR\alpha}$ and G_{SWS} values are shown in Fig. 11 as the experimental shear modulus of SW. According to the regression curves of $G_{SWR\alpha}$ and G_{SWS} (solid lines), the experimental shear moduli of SW (0.35–0.40 g/cm^3) were 73–89 and 109–125 MPa/rad, respectively. The theoretical shear modulus of SW (0.35–0.40 g/cm^3) was 110–129 MPa/rad. Based on $G_{SWR\alpha}$ and G_{SWS}, respectively, the shear moduli of SW are about 1.8–2.4 times and 2.6–3.7 times higher than that of the core, referring to $G_{FB\alpha}$ (0.28–0.33 g/cm^3, 30–49 MPa/rad).

In this connection, the calculated shear modulus of the structural panel composite, which consists of a pair of nailed structural plywood specimens of 9 mm thickness with a full-scale shear wall size, is 106 MPa/rad.[20] The shear modulus of SW matches it, though they cannot be compared exactly.

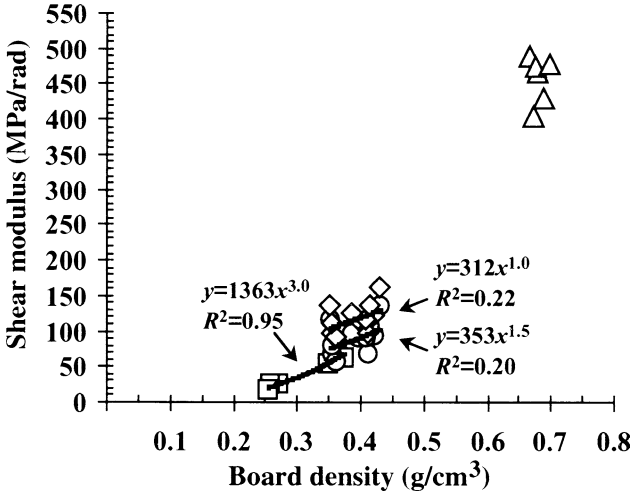

Fig. 11. Experimental shear moduli of SW evaluated by $G_{SWR\alpha}$ (*open circles*) and G_{SWS} (*open diamonds*), compared with the shear moduli of PW and FB evaluated by $G_{PW\alpha}$ (*open triangles*) and $G_{FB\alpha}$ (*open squares*), respectively. *Solid lines*, regression curves for $G_{SWR\alpha}$, G_{SWS}, and $G_{FB\alpha}$

Fig. 12. Example of the ultimate stage of shear failure of SW. The direction of the surface grain of the face plywood is perpendicular to the loading direction. The density of the specimen is 0.41 g/cm^3. Both face and core were crushed by the shearing stress. The fracture occurred around the neutral surface of the test specimen

Shear strength

Figure 12 shows a typical shear failure appearance of SW. Shear failure occurred in all of the other specimens of SW as well as PW and FB.

The shear strength (τ) of SW was defined as the maximum load divided by the shear area. The τ is indicated in relation to board density in Fig. 13. The effect of the setting direction on τ was not significant. The effects of the fastener type on τ were negligible. There was no reduction of the τ value for SW under the PPC load compared to that under the MP load. A similar trend was observed in the τ values for PW and FB.

Without recognizing the setting direction and fastener type, the trends can be summarized as follows. As the τ of SW depended on board density, the regression curve of involution function was fitted to SW ($y = 6.5x^{1.6}$, $R^2 = 0.61$). According to this calculation, the τ of SW (0.35–0.40 g/cm^3) was 1.2–1.5 MPa. The average τ of PW (0.68 g/cm^3) was 4.6 MPa. As the τ of FB depended on board density, the regression curves of involution function were fitted ($y = 4.0x^{1.9}$, $R^2 = 0.87$). Therefore, the τ of FB (0.25–0.35 g/cm^3) was 0.29–0.54 MPa.

The τ of SW at densities of 0.35 and 0.40 g/cm^3 were 3.4 and 3.1 times higher than those in the core, with densities of 0.28 and 0.33 g/cm^3 (0.36 and 0.49 MPa), respectively. They were one-fourth and one-third the τ of PW, respectively.

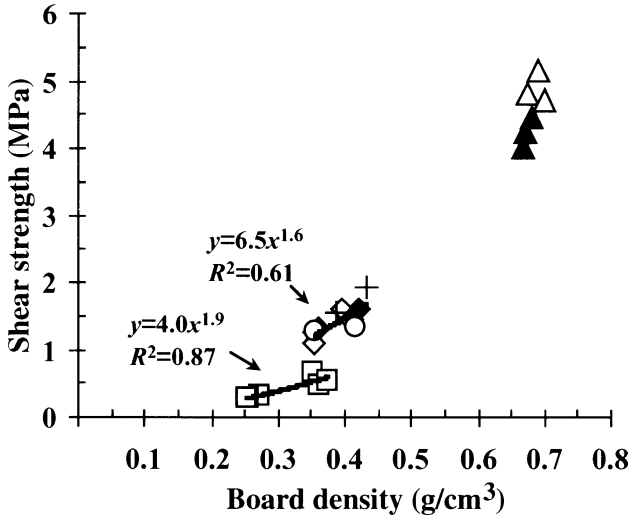

Fig. 13. Shear strength of SW (*open circles*, type 1; *crosses*, types 2, 3; *filled diamonds*, type 4; *open diamonds*, type 5), of PW (*filled triangles*, type 6; *open triangles*, type 7), and of FB (*open squares*, type 8). *Solid lines*, regression curves for SW and FB. Refer to Table 1 for the fastener type

Conclusions

The shear test method using tie-rods for the general shear wall was useful for investigating the fundamental shear behavior of SW as a small shear wall. The shear modulus must be carefully determined in low-density fiberboard and sandwich panels. Knowledge about the shear behavior of SW can provide a basis for the development of wood-based sandwich panels as practical shear walls.

Acknowledgments The authors express our deep gratitude to Mr. Noritoshi Sawada (Hokushin Co.), Dr. Wong Cheng, and their cooperative members for their expert technical support for the preparation of manufacturing the thick fiberboard and sandwich panel. We are grateful also to Drs. Min Zhang, Kenji Umemura, Wong Ee Ding, and Guangping Han for their great help and advice in manufacturing the thick panels. The authors are grateful to Hokushin Co. for the fiber and resin and to Ishinomaki Gouhan Co. for the plywood. We thank Mr. Makoto Nakatani for his expert assistance when preparing the specimens for the shear test. Funding provided by the Research Fellowship of the Japan Society for the Promotion of Science for Young Scientists as a JSPS Research Fellow is also gratefully acknowledged.

References

1. Jack RV (1999) The behavior of sandwich structures of isotropic and composite materials. Technomic Publishing, Lancaster, PA, USA
2. Gibson LJ, Ashby MF (1997) The design of sandwich panels with foam cores. In: Clarke DR, Suresh S, Ward FRSIM (eds) Cellular solids. Cambridge University Press, Cambridge
3. Kawasaki T, Zhang M, Kawai S (1998) Manufacture and properties of ultra-low density fiberboard. J Wood Sci 44:354–360
4. Kawasaki T, Zhang M, Kawai S (1999) Sandwich panel of veneer-overlaid low-density fiberboard. J Wood Sci 45:291–298
5. Japanese Industrial Standard (1994) JIS A 1414–1973 Methods of performance test of panels for building construction. Japanese Standard Association, Tokyo
6. Japanese Agricultural Standard (1999) JAS for structural plywood. Ministry of Agriculture, Forestry and Fisheries, Tokyo
7. Sasaki H (1990) Development of continuous press with steam-injection heating from both sides. Report of the grants-in-aid for scientific research (no. 01860023) from the Ministry of Education, Science and Culture, Japan
8. American Society of Testing and Materials (1996) D2719-89 standard test methods for structural panels in shear through-the-thickness. In: 1996 Annual book of ASTM standards. ASTM, Philadelphia
9. American Society of Testing and Materials (1996) D1037-96 standard test methods for evaluating properties of wood-base fiber and particle panel materials. In: 1996 Annual book of ASTM standards. ASTM, Philadelphia
10. Okuma M (1961) Shearing modulus of plywood and hardboard measured by the panel shear test. I. Measuring of shearing modulus by the ASTM method (in Japanese). Mokuzai Gakkaishi 7:242–246
11. Okuma M (1962) Shearing modulus of plywood and hardboard measured by the panel shear test. II. Investigations on the form of the load-strain curve (in Japanese). Mokuzai Gakkaishi 8:54–58
12. Okuma M (1962) Shearing modulus of plywood and hardboard measured by the panel shear test. III. Measuring of shear modulus by the improved Larsson-Wästlund method (in Japanese). Mokuzai Gakkaishi 8:58–61
13. Takami I (1964) Panel and plate shear test for plywood (in Japanese). Mokuzai Gakkaishi 10:1
14. Sasaki H, Maku T (1964) Strain distribution on plywood panel shear test specimens (in Japanese). Mokuzai Kenkyu 33:37–46
15. Okuma M, Shida S, Ohhashi M (1983) Manufacture and performance of radiata pine plywood. I (in Japanese). Mokuzai Gakkaishi 29:438–443
16. Suzuki S, Nawa D, Miyamoto K, Shibusawa T (2000) Shear-through-thickness properties of wood-based panels determined by the two-rail shear and edgewise shear methods. J Soc Mater Sci 49:395–400
17. Lee AWC, Stephens CB (1988) Comparative shear strength of seven types of wood composite panels at high and medium relative humidity conditions. For Prod J 38(3):49–52
18. Wong ED (1999) Density profile: its formation and effects on the properties of particleboard and fiberboard. Dissertation, Department of Forest and Biomass Science, Graduate School of the Faculty of Agriculture, Kyoto University, pp 69–70
19. Nihon Jutaku Mokuzai Technical Center (1989) The information for the design of the three-storied wooden house construction and fire resistance (in Japanese). Ministry of Construction, Tokyo, pp 15–21
20. Notification No.1100 of the Ministry of Construction of Japan, 1981